RAA 2017 Vol. **17** No. **9**, 94 (10pp) doi: 10.1088/1674–4527/17/9/94

http://www.raa-journal.org *http://iopscience.iop.org/raa*

***R**esearch in*
***A**stronomy and*
***A**strophysics*

Study of photometric phase curve: assuming a cellinoid ellipsoid shape for asteroid (106) Dione

Yi-Bo Wang[1,2,3], Xiao-Bin Wang[1,3,4], Donald P. Pray[5] and Ao Wang[1,2,3]

[1] Yunnan Observatories, Chinese Academy of Sciences, Kunming 650216, China; *wangyb@ynao.ac.cn, wangxb@ynao.ac.cn*
[2] University of Chinese Academy of Sciences, Beijing 100049, China
[3] Key Laboratory for the Structure and Evolution of Celestial Objects, Chinese Academy of Sciences, Kunming 650216, China
[4] Center for Astronomical Mega-Science, Chinese Academy of Sciences, Beijing 100012, China
[5] Sugarloaf Mountain Observatory, South Deerfield, MA 01373, USA

Received 2017 May 9; accepted 2017 May 31

Abstract We carried out new photometric observations of asteroid (106) Dione at three apparitions (2004, 2012 and 2015) to understand its basic physical properties. Based on a new brightness model, new photometric observational data and published data of (106) Dione were analyzed to characterize the morphology of Dione's photometric phase curve. In this brightness model, a cellinoid ellipsoid shape and three-parameter (H, G_1, G_2) magnitude phase function system were involved. Such a model can not only solve the phase function system parameters of (106) Dione by considering an asymmetric shape of an asteroid, but also can be applied to more asteroids, especially those without enough photometric data to solve the convex shape. Using a Markov Chain Monte Carlo (MCMC) method, Dione's absolute magnitude of $H = 7.66^{+0.03}_{-0.03}$ mag, and phase function parameters $G_1 = 0.682^{+0.077}_{-0.077}$ and $G_2 = 0.081^{+0.042}_{-0.042}$ were obtained. Simultaneously, Dione's simplistic shape, orientation of pole and rotation period were also determined preliminarily.

Key words: asteroids: general: photometric phase curve — asteroids: individual: (106) Dione — techniques: photometric — Markov Chain Monte Carlo method

1 INTRODUCTION

Asteroids are thought to be the remnants of planetesimals related to the progenitor bodies which formed terrestrial planets and cores of giant planets. They can provide us with important clues on the pristine composition of the solar nebula (Michel et al. 2015).

A photometric phase curve, as one of the crucial physical properties of an asteroid, represents the observational brightness variations at different solar phase angles (hereafter called phase angles). It can also provide us with important information on the nature of the surface of an asteroid, such as porosity, asymmetry factor and roughness (Hapke 1984, 1986, 2002; Muinonen 1994; Dlugach & Mishchenko 1999, 2013; Belskaya & Shevchenko 2000; Muinonen et al. 2002; Oszkiewicz et al. 2012).

In 1985, a semi-empirical $H - G$ magnitude system (Bowell et al. 1989) was adopted as the standard magnitude system by the International Astronomical Union (IAU), where H and G are the absolute magnitude of an asteroid and the slope factor, respectively. This $H - G$ magnitude system originating from the Lumme-Bowell theory (Lumme & Bowell 1981) has been used to study the behavior of the photometric phase curves of asteroids for many years. However, it cannot accurately fit the photometric phase curves of exceptionally low-albedo or high-albedo asteroids (Belskaya & Shevchenko

2000). Therefore, a three-parameter (H, G_1, G_2) magnitude phase function system (Muinonen et al. 2010) was adopted as the new standard magnitude system in the 28th General Assembly of the IAU. This new system improves the fitting results of photometric phase curves for taxonomy of asteroids (Muinonen et al. 2010; Oszkiewicz et al. 2012; Penttilä et al. 2016; Shevchenko et al. 2016). The parameters G_1 and G_2, to some extent, can also be used to infer information about the surface material of small objects in the solar system, especially for distant small objects.

In order to study the photometric phase curve of an asteroid, observational data derived in a large range of phase angles are needed. However, a sufficient amount of data is difficult to obtain with ground-based instruments in a single apparition, due to weather conditions and constraints on observation time. For observational data obtained during different apparitions, due to the effect of the non-spherical shape of an asteroid, the phase function system parameters will be changed with varying geometries of observation.

A brightness model has been used to estimate the phase function system parameters of (107) Camilla by considering a tri-axial ellipsoid shape and the (H, G_1, G_2) magnitude phase function system in our previous work (Wang et al. 2016). However, this simple tri-axial ellipsoid cannot be applied appropriately to asteroids with an irregular shape.

In this paper, we develop a new brightness model which can more accurately estimate the magnitude-phase relation, rotation period, orientation of pole and simplistic shape of an asteroid. In detail, we consider an asymmetric shape model, a cellinoid ellipsoid (Cellino et al. 1989; Lu et al. 2014), consisting of eight adjacent octants of an ellipsoid with different semi-axes $(a_1, a_2, b_1, b_2, c_1, c_2)$ in this new brightness model, which allows for a better fit to an asteroid with an irregular shape. In addition, the three-parameter (H, G_1, G_2) magnitude phase function system is also used.

We applied the new brightness model to analyze photometric data of the main-belt asteroid (106) Dione. The photometric observational data of asteroid (106) Dione have been obtained by several groups (Harris et al. 1992; Pray 2005). Harris et al. (1992) and Pray (2005) obtained different rotation periods (15 h vs. 16.26 h). In addition, Harris et al. (1992) firstly estimated the absolute magnitude of Dione to be $H = 7.41$ mag by assuming a slope factor $G = 0.09$. Later, Shevchenko & Tedesco (2006) obtained its absolute magnitude to be $H = 7.66$ mag by occultation data. However, until now, detailed information on Dione's orientation of pole and shape has not been obtained. In order to accurately determine the phase function system parameters, spin parameters and shape of Dione, new observations at three apparitions (2004, 2012 and 2015) were carried out with the 1.0-m telescope administered by Yunnan Observatories (IAU Observatory Code 286).

Section 2 describes the observation and data reduction of asteroid (106) Dione. In Section 3, we introduce the new brightness model and the Markov Chain Monte Carlo (MCMC) method. The result of applying this model to (106) Dione is presented in Section 4 and the discussion is contained in Section 5. Finally, in the last section we conclude this work.

2 OBSERVATION AND DATA REDUCTION

To understand the basic physical properties of (106) Dione, we carried out photometric observations with the 1-m telescope administered by Yunnan Observatories in 2004, 2012 and 2015. The photometric observational data of (106) Dione in 2004 were gathered by the 1k×1k pixel PI 1024TKB CCD camera with a field of view (FOV) of $6.5' \times 6.5'$; the data in 2012 and 2015 were obtained by the 2k×2k pixel Andor DW436 CCD camera with an FOV of $7.3' \times 7.3'$.

All the scientific images were reduced using the Image Reduction and Analysis Facility (IRAF) software. Following the standard reduction process, bias and flat field effects were corrected on the scientific images. Occasional cosmic rays hits in these images were identified by a criterion of four times the standard deviation of sky background and then were removed. Utilizing the APPHOT task, the instrumental magnitudes of reference stars and the target asteroid are measured by an optimal aperture.

Before the photometric phase curve of asteroid (106) Dione could be analyzed, the instrumental magnitudes of the asteroid needed to be converted into the standard photometry system (e.g. the Landolt standard photometry system). The procedure of magnitude calibration contains two steps: (1) Obtain the transformation relation between the instrument magnitude $m_{\rm obs}$ and the magnitude r' from the Carlsberg Meridian Catalogue (CMC 15) system (Muiños & Evans 2014) by reference stars in the observed images,

$$m_{\rm obs} = k(J - K) + r' + m_0, \qquad (1)$$

where the examined parameters k and m_0 are solved by the linear least squares method. J- and K-band magnitudes are derived from the 2MASS catalog. Then, the magnitudes of the asteroid in the CMC 15 photometry system are obtained by this transformation relation. (2) Convert these magnitudes into the Landolt standard photometry system in terms of the relation given by Dymock & Miles (2009),

$$V = 0.6278(J - K) + 0.9947r'. \quad (2)$$

For asteroid (106) Dione, a mean value $J - K = 0.407$ is adopted in this calibration procedure, which is derived from 61 asteroids with a similar spectral type in the 2MASS Asteroid and Comet Survey V2.0 (Sykes et al. 2010). The time stamps of observed data were corrected by the light-time.

Information on our new observations is listed in Table 1, which includes the middle date of the span of observations in UT, the heliocentric distance r and the geocentric distance Δ in AU, the phase angle α, the filter and the instrument used during the observations. Besides our new observational data, existing data which have been published are also incorporated in our study, and observational information on these data is listed in Table 2. In total, observations of (106) Dione acquired over 26 nights are involved, and all lightcurves are shown in Figure 1.

3 THEORETICAL AND NUMERICAL METHODS

3.1 Brightness Model

The photometric phase curve contains information on the absolute magnitude and surface material properties. In early studies of the magnitude-phase relation, a spherical shape of the asteroid was assumed. In fact, the shapes of most asteroids are irregular. The observed brightness of an asteroid with an irregular shape would inevitably vary due to changes in the illuminated and viewed areas, when the geometries of observations vary in different apparitions. In order to determine the phase function system parameters accurately, a new brightness model considering the effect of an irregular shape is developed as follows,

$$V(1, 1, \alpha) = f(\alpha) + 2.5\log_{10}(\delta), \quad (3)$$

where $V(1, 1, \alpha)$ represents the reduced magnitude, which is corrected by considering the effect of asteroid-Earth and asteroid-Sun distances in terms of the relation from Bowell et al. (1989, equation (A2)); α is the phase angle and $f(\alpha)$ is a certain magnitude-phase dependence. At present, the three-parameter (H, G_1, G_2) magnitude phase function system (Muinonen et al. 2010; Penttilä et al. 2016) is adopted as follows,

$$f(\alpha) = H - 2.5\log_{10}\Big[G_1\phi_1(\alpha) + G_2\phi_2(\alpha) + (1 - G_1 - G_2)\phi_3(\alpha)\Big], \quad (4)$$

where phase functions $\phi_1(\alpha)$, $\phi_2(\alpha)$ and $\phi_3(\alpha)$ are defined by Muinonen et al. (2010) and Penttilä et al. (2016). In addition, H is absolute magnitude; G_1 and G_2 are phase function parameters.

In Equation (3), δ represents the observed brightness difference of reflected sunlight between the asteroid and its equivalent sphere, which can be described as follows,

$$\delta = \frac{L^*}{L}, \quad (5)$$

where L^* and L represent observed integral luminosity of reflected sunlight of this equivalent sphere and the asteroid, respectively. In this work, an asymmetric shape model, the cellinoid ellipsoid (Cellino et al. 1989; Lu et al. 2014), is adopted to roughly simulate the shape of the asteroid. The cellinoid ellipsoid shape model, as shown in Figure 2, consists of eight adjacent octants of an ellipsoid with different semi-axes $(a_1, a_2, b_1, b_2, c_1, c_2)$ which are restricted by,

$$\begin{aligned} a_1 + a_2 &= 2a, \\ b_1 + b_2 &= 2b, \\ c_1 + c_2 &= 2c. \end{aligned} \quad (6)$$

In order to approximately estimate L, the surface of this cellinoid ellipsoid is divided into several small triangular plane facets, and each triangular plane facet consists of three given vertices. For any vertex in this triangular plane facet, its vector $\boldsymbol{r}(x, y, z)$ is restricted by,

$$\frac{x^2}{a_l^2} + \frac{y^2}{b_m^2} + \frac{z^2}{c_k^2} = 1, (l = 1, 2; m = 1, 2; k = 1, 2). \quad (7)$$

Therefore, for the given triangular plane facet, its area $\Delta\sigma$ can be calculated by the vectors $(\boldsymbol{r}_1, \boldsymbol{r}_2, \boldsymbol{r}_3)$ of three given vertices. In this analysis, the asteroid is assumed to rotate about a principal axis passing through its center of mass. For each vertex on the surface of the cellinoid ellipsoid, the coordinate transformation relation between the vector $\boldsymbol{r}_{\rm ast}$ in the co-rotating coordinate frame of the asteroid and the vector $\boldsymbol{r}_{\rm ecl}$ in the ecliptic coordinate frame

Table 1 Information on the New Photometric Observations of Asteroid (106) Dione

Date (UT)	r (AU)	Δ (AU)	α (°)	Filter	Note
2004/11/03.8	2.684	1.830	13.1	I	1.0-m YNAO
2004/11/04.8	2.685	1.824	12.7	V, I	1.0-m YNAO
2004/11/06.9	2.687	1.810	12.0	I	1.0-m YNAO
2004/11/07.8	2.688	1.804	11.6	I	1.0-m YNAO
2004/11/08.9	2.689	1.798	11.3	I	1.0-m YNAO
2004/12/01.8	2.714	1.730	1.8	I	1.0-m YNAO
2004/12/03.8	2.716	1.731	1.0	V, I	1.0-m YNAO
2012/03/13.7	3.578	2.591	2.1	R	1.0-m YNAO
2012/03/14.7	3.579	2.590	1.9	R	1.0-m YNAO
2012/03/15.8	3.580	2.590	1.8	R	1.0-m YNAO
2012/03/17.8	3.582	2.590	1.6	R	1.0-m YNAO
2015/11/15.6	2.651	1.694	6.8	C	1.0-m YNAO
2015/11/16.6	2.651	1.698	7.2	C	1.0-m YNAO

Table 2 Information on the Photometric Observations of Asteroid (106) Dione Derived from Published Literatures

Date (UT)	r (AU)	Δ (AU)	α (°)	Filter	Reference
1981/09/20.3	2.626	1.655	7.1	V	Harris et al. (1992)
1981/09/22.3	2.624	1.647	6.3	V	Harris et al. (1992)
1981/09/27.2	2.621	1.630	4.3	V	Harris et al. (1992)
2004/12/04.3	2.717	1.731	0.8	C	Pray (2005)
2004/12/06.2	2.719	1.734	0.6	C	Pray (2005)
2004/12/09.2	2.722	1.739	1.7	C	Pray (2005)
2004/12/15.2	2.729	1.758	4.2	C	Pray (2005)
2004/12/16.1	2.730	1.762	4.6	C	Pray (2005)
2004/12/18.2	2.733	1.772	5.5	C	Pray (2005)
2004/12/21.2	2.737	1.788	6.7	C	Pray (2005)
2004/12/31.1	2.749	1.856	10.5	C	Pray (2005)
2005/01/02.1	2.751	1.872	11.2	C	Pray (2005)
2005/01/11.2	2.763	1.960	14.0	C	Pray (2005)

can be obtained as follows,

$$\boldsymbol{r}_{\rm ast} = R_z\left[\Phi_0 + \frac{360^\circ}{P}(t-t_0)\right] R_y[90^\circ - \beta_p] \\ R_z[\lambda_p]\boldsymbol{r}_{\rm ecl}, \tag{8}$$

where R_y and R_z are the standard rotation matrixes; (λ_p,β_p) is the orientation of the pole, P is the rotation period and Φ_0 is the initial rotation phase angle. In addition, t_0 and t represent the zero time and the observation time, respectively.

Therefore, based on the combined form of the Lommel-Seeliger law and the Lambert law (Kaasalainen et al. 2001), L is calculated as follows,

$$\begin{cases} L \approx \sum\limits_{i,j} S(\mu^{i,j}, \mu_0^{i,j})\Delta\sigma_{i,j}, \\ S(\mu^{i,j}, \mu_0^{i,j}) = \dfrac{\mu^{i,j}\mu_0^{i,j}}{\mu^{i,j} + \mu_0^{i,j}} + C\mu^{i,j}\mu_0^{i,j}, \end{cases} \tag{9}$$

where i and j are the indexes of the given small triangular plane facet; $\mu_0^{i,j}$ and $\mu^{i,j}$ are cosines of angles of incidence and reflection respectively,

$$\begin{aligned} \mu_0^{i,j} &= \cos\left(\boldsymbol{n}(i,j)\cdot\mathbf{Sun}\right), \\ \mu^{i,j} &= \cos\left(\boldsymbol{n}(i,j)\cdot\mathbf{observer}\right), \end{aligned} \tag{10}$$

where $\boldsymbol{n}(i,j)$ represents the outward normal direction of the given triangular plane facet. In the calculation process of L, each triangular plane facet should be illuminated by sunlight and be visible by observers, simultaneously. Thus, the criterion must be fulfilled as follows,

$$\mu_0^{i,j} > 0, \qquad \mu^{i,j} > 0, \tag{11}$$

otherwise $S(\mu^{i,j}, \mu_0^{i,j}) = 0$ in Equation (9). Furthermore, in Equation (5), L^* has a mathematical form similar to L. Finally, δ is a function of these parameters: orientation of pole (λ_p, β_p), axial ratios of

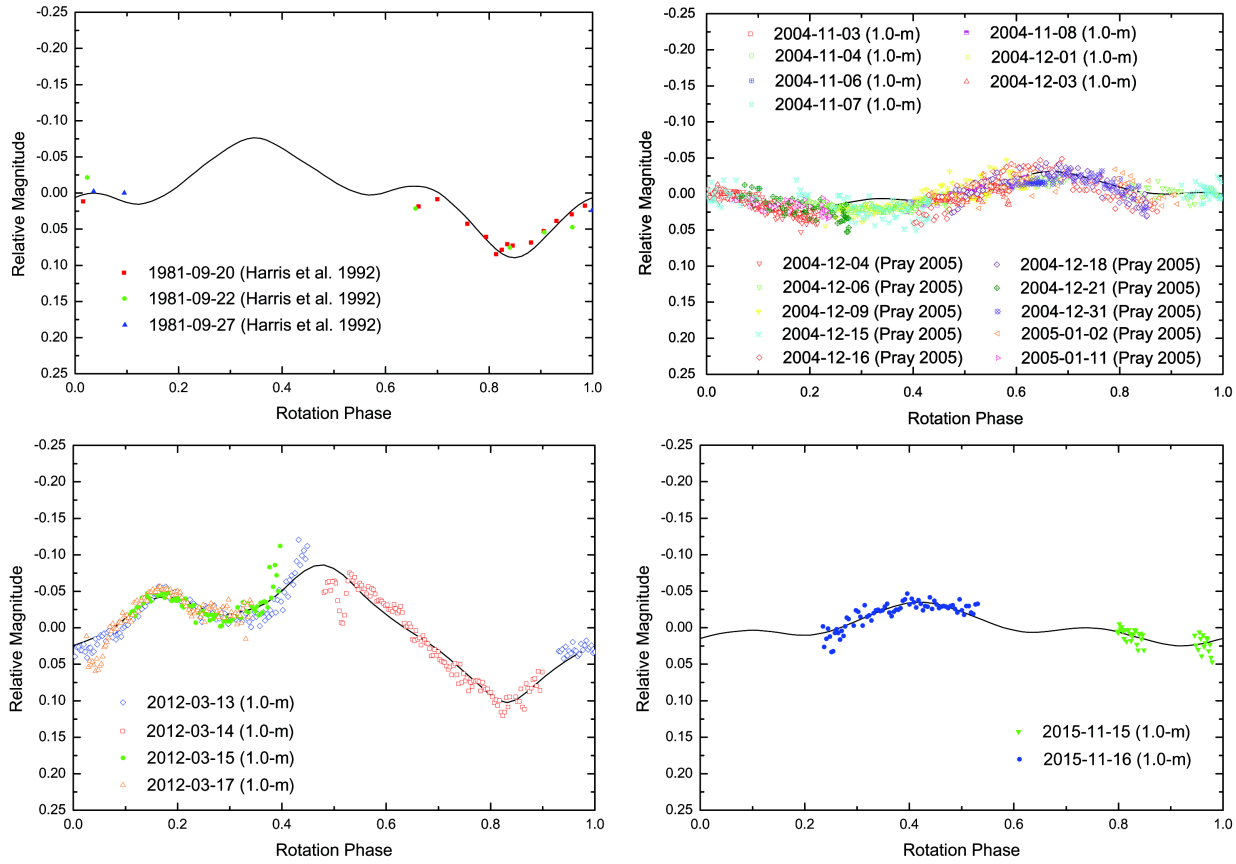

Fig. 1 Lightcurves of asteroid (106) Dione with the rotation period $P = 16.2345$ h. The zero time t_0 is set at JD 2453313.29363 for all observational data and the solid lines are modeled lightcurves given by the applied cellinoid ellipsoid in this figure.

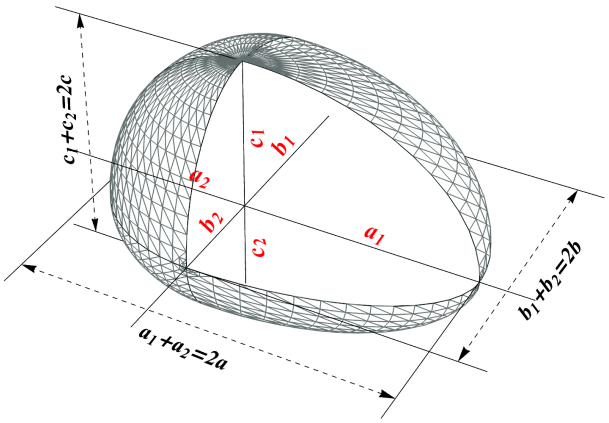

Fig. 2 Cellinoid ellipsoid model.

cellinoid ellipsoid shape $(a/b, b/c, a_1/a, b_1/b, c_1/c)$, rotation period P, initial rotation phase angle Φ_0 and weight factor C.

Suppose $V_{i,j}^{\rm obs}$ denotes the j-th observed data point in the i-th lightcurve and $V_{i,j}^{\rm model}$ represents that calculated by Equation (3). The chi-square χ^2 can be obtained by

$$\chi^2 = \sum_i \sum_j \frac{\|V_{i,j}^{\rm obs} - V_{i,j}^{\rm model}\|^2}{\sigma_{i,j}^2}. \qquad (12)$$

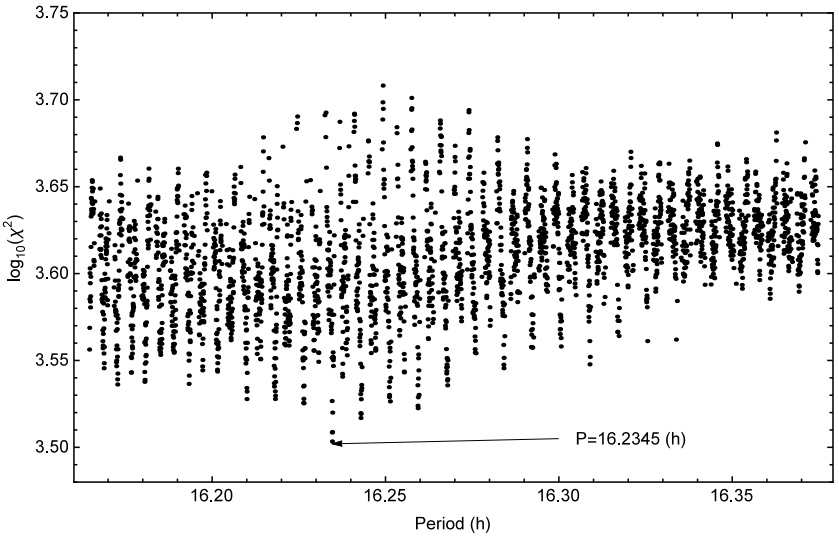

Fig. 3 The distribution of period of (106) Dione vs. $\log_{10}(\chi^2)$ for the model fits of lightcurves.

In practical analysis, a mean uncertainty $\overline{\sigma}$ can be used to substitute for the observational error $\sigma_{i,j}$ in Equation (12).

3.2 Markov Chain Monte Carlo Method

According to Bayes' theorem, the basic equation is as follows,

$$P(\Theta|y) = \frac{P(y|\Theta)P(\Theta)}{P(y)}, \tag{13}$$

where Θ is the unknown parameter vector and y represents the observed data; $P(y|\Theta)$ is a probability reflecting how the given parameter Θ fits the observational data y, and $P(\Theta)$ is the prior probability. In this new brightness model introduced in Section 3.1, 13 unknown parameters are involved: absolute magnitude H, phase function parameters G_1 and G_2, rotation period P, initial rotation phase angle Φ_0, orientation of pole (λ_p, β_p), axial ratios of cellinoid ellipsoid $(a/b, b/c, a_1/a, b_1/b, c_1/c)$ and weight factor C. Therefore, the unknown parameter vector can be represented by $\Theta = (H, G_1, G_2, P, \Phi_0, \lambda_p, \beta_p, a/b, b/c, a_1/a, b_1/b, c_1/c, C)$. In order to estimate the optimized fitting values of these parameters, an MCMC method (Collier Cameron et al. 2007; Muinonen et al. 2009) is adopted in this work. Thus, based on a classical Metropolis-Hastings method (Gilks et al. 1996), a posterior probability density function is sampled in,

$$p(\Theta) \propto \exp\left[-\frac{\chi^2(\Theta)}{2}\right]. \tag{14}$$

For the probability density function $q(\Theta, \Theta_i)$, a new set of unknown parameters is accepted, namely $\Theta_{i+1} = \Theta$, if the acceptance criterion is fulfilled as,

$$u < \frac{p(\Theta)q(\Theta, \Theta_i)}{p(\Theta_i)q(\Theta_i, \Theta)}, \tag{15}$$

otherwise the set of unknown parameters remains unchanged, namely $\Theta_{i+1} = \Theta_i$. In Equation (15), u represents a random deviate which fulfills $u \in [0, 1]$. If q is symmetric, Muinonen et al. (2009) suggest a simple acceptance criterion form as follows,

$$u < \frac{p(\Theta)}{p(\Theta_i)}. \tag{16}$$

For practical application of MCMC processes in this work, a symmetric Gaussian probability density function is adopted for each parameter in the probability density function $q(\Theta, \Theta_i)$. Using this MCMC method, the best-fit values and uncertainties of all 13 unknown parameters are estimated.

4 RESULTS

In order to determine the orientation of pole and shape, an accurate rotation period is searched by setting a tentative shape and orientation of pole.

Figure 3 shows the distribution of period vs. $\log_{10}(\chi^2)$. The optimal rotation period of 16.2345 h and an initial rotation phase angle $\Phi_0 = 160^\circ$ are obtained. This period and the initial rotation phase angle will be taken as the initial values in the following steps.

In order to analyze the photometric phase curve accurately, all the calibrated photometric data are used.

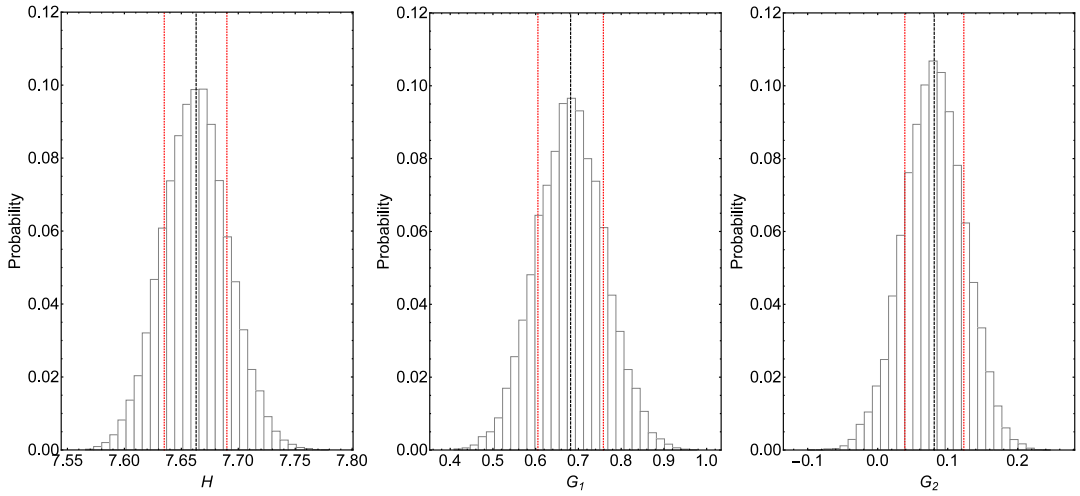

Fig. 4 The posterior probability distributions of parameters H, G_1 and G_2 for (106) Dione from left to right respectively. The black dash-dotted lines show the best values, and the interval between the two red lines denotes the $1-\sigma$ uncertainty in each panel.

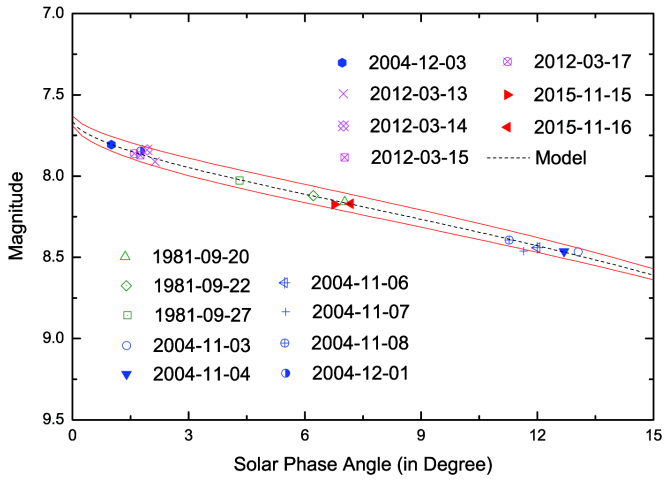

Fig. 5 New photometric phase curve of asteroid (106) Dione (*black dashed line*) with $1-\sigma$ error envelopes (*red lines*).

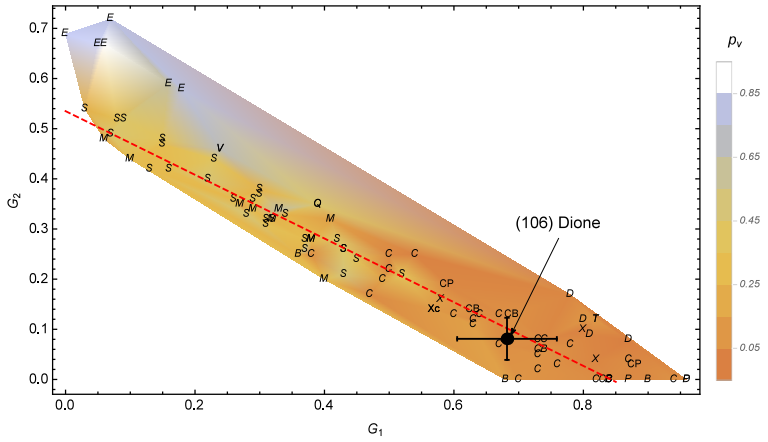

Fig. 6 The relation between parameters G_1 and G_2, and the distribution of albedo p_v based on the results of Shevchenko et al. (2016). The solid black circle with $1-\sigma$ error bars is the result of (106) Dione.

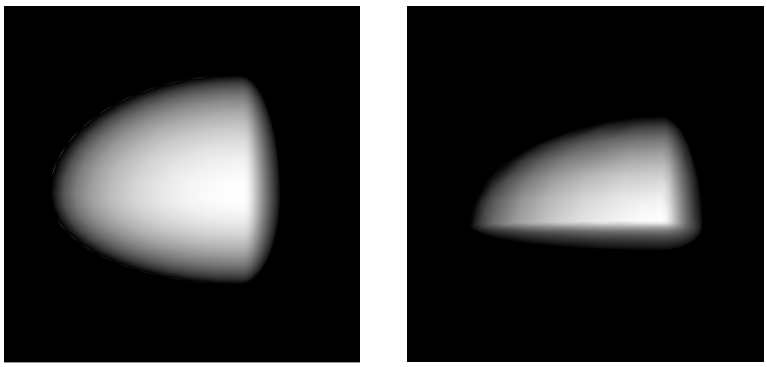

Fig. 7 The cellinoid ellipsoid model of asteroid (106) Dione shown from c-axis viewing (*left*) and from b-axis viewing (*right*).

Utilizing the MCMC method introduced in Section 3.2, the 13 unknown parameters of asteroid (106) Dione are obtained in this new brightness model.

Figure 4 shows the posterior probability distributions of parameters H, G_1 and G_2. The optimal values and uncertainties of these parameters are estimated: absolute magnitude $H = 7.66^{+0.03}_{-0.03}$ mag, and phase function parameters $G_1 = 0.682^{+0.077}_{-0.077}$ and $G_2 = 0.081^{+0.042}_{-0.042}$. The new photometric phase curve of asteroid (106) Dione is shown in Figure 5. The photometric phase curves associated with different taxonomies of asteroids were analyzed by Oszkiewicz et al. (2012), Penttilä et al. (2016) and Shevchenko et al. (2016), and the relation between phase function parameters G_1 and G_2 and albedo p_v was discussed by Shevchenko et al. (2016). For the results of (106) Dione as shown in Figure 6, it is evident that the G_1 and G_2 values found by this new model are in agreement with the typical values for dark asteroids. Furthermore, Dione's spin parameters and cellinoid shape are also obtained: rotation period $P = 16.2345^{+0.0001}_{-0.0001}$ h, initial rotation phase angle $\Phi_0 = 168.8^{\circ+8.2}_{-8.0}$, orientation of pole $(58.0^{\circ+4.5}_{-4.9}, 21.1^{\circ+6.1}_{-6.0})$, axial ratios of cellinoid ellipsoid shape ($a/b = 1.10^{+0.02}_{-0.01}, b/c = 1.59^{+0.07}_{-0.06}, a_1/a = 1.65^{+0.03}_{-0.03}, b_1/b = 0.86^{+0.01}_{-0.01}, c_1/c = 1.64^{+0.03}_{-0.04}$) and weight factor $C = 0.29^{+0.03}_{-0.03}$. The simplistic ellipsoid shape of asteroid (106) Dione is shown in Figure 7. In addition, due to the data not uniquely restricting the orientation of pole, another solution with a different longitude of the pole near $\lambda_p + 180^\circ$ can exist. Based on the new brightness model, the other possible absolute magnitude $H = 7.66^{+0.03}_{-0.03}$ mag, and phase function parameters $G_1 = 0.687^{+0.082}_{-0.081}$ and $G_2 = 0.073^{+0.039}_{-0.042}$ are obtained with $P = 16.2345^{+0.0001}_{-0.0001}$ h, $\Phi_0 = 156.5^{\circ+7.7}_{-7.2}$, orientation of pole $(242.5^{\circ+4.2}_{-4.0}, 21.5^{\circ+6.3}_{-6.8})$, axial ratios of shape ($a/b = 1.10^{+0.01}_{-0.01}, b/c = 1.59^{+0.08}_{-0.08}, a_1/a = 0.35^{+0.03}_{-0.03}, b_1/b = 1.14^{+0.01}_{-0.01}, c_1/c = 0.36^{+0.03}_{-0.03}$) and $C = 0.29^{+0.03}_{-0.03}$. The fitting results and uncertainties of all unknown parameters of asteroid (106) Dione are listed in Table 3.

5 DISCUSSION

(106) Dione is a main belt asteroid with low albedo. Published photometric data on (106) Dione were obtained by Harris et al. (1992) and Pray (2005). A rough rotation period of 15 h was estimated by Harris et al. (1992) through observations acquired over three nights, however a significantly different period of 16.26 h was obtained by Pray (2005). Therefore, a more accurate rotation period needs to be redetermined. By adding new photometric observational data, Dione's rotation period of 16.2345 h is determined in our analysis, and it is notable that the period derived by Pray (2005) may be a local minimum solution, which can be seen in Figure 3.

In addition, the orientation of pole and shape of (106) Dione have been never determined. Utilizing the observational data listed in Tables 1 and 2, the orientation of pole $(58.0^\circ, 21.1^\circ)$ of Dione is obtained, and moreover it is evident that Dione has quite an asymmetric shape ($a/b = 1.10$, $b/c = 1.59$, $a_1/a = 1.65$, $b_1/b = 0.86$ and $c_1/c = 1.64$) as shown in Figure 7.

For the phase function system parameters of (106) Dione, Harris et al. (1992) estimated an absolute magnitude of $H = 7.41$ mag which was obtained by observational data acquired over three nights in the 1981 apparition and by assuming a mean slope factor of $G = 0.09$ for dark asteroids. Values for the phase angle of these observations were distributed in a range from 4° to 8°. It is obvious that these parameters are difficult to use to describe the morphology of the photometric phase curve of asteroid (106) Dione well. Therefore, more efficient ob-

Table 3 The Estimated Parameters of Asteroid (106) Dione

Parameter	Pole 1	Pole 2
H	$7.66^{+0.03}_{-0.03}$	$7.66^{+0.03}_{-0.03}$
G_1	$0.682^{+0.077}_{-0.077}$	$0.687^{+0.082}_{-0.081}$
G_2	$0.081^{+0.042}_{-0.042}$	$0.073^{+0.039}_{-0.042}$
P	$16.2345^{+0.0001}_{-0.0001}$	$16.2345^{+0.0001}_{-0.0001}$
Φ_0	$168.8^{\circ}{}^{+8.2}_{-8.0}$	$156.5^{\circ}{}^{+7.7}_{-7.2}$
λ_p	$58.0^{\circ}{}^{+4.5}_{-4.9}$	$242.5^{\circ}{}^{+4.2}_{-4.0}$
β_p	$21.1^{\circ}{}^{+6.1}_{-6.0}$	$21.5^{\circ}{}^{+6.3}_{-6.8}$
a/b	$1.10^{+0.02}_{-0.01}$	$1.10^{+0.01}_{-0.01}$
b/c	$1.59^{+0.07}_{-0.06}$	$1.59^{+0.08}_{-0.08}$
a_1/a	$1.65^{+0.03}_{-0.03}$	$0.35^{+0.03}_{-0.03}$
b_1/b	$0.86^{+0.01}_{-0.01}$	$1.14^{+0.01}_{-0.01}$
c_1/c	$1.64^{+0.03}_{-0.04}$	$0.36^{+0.03}_{-0.03}$
C	$0.29^{+0.03}_{-0.03}$	$0.29^{+0.03}_{-0.03}$

servational data are needed to estimate these phase function system parameters. However, it can be noted that an asymmetric shape of (106) Dione significantly deviates from a sphere. Thus, serious uncertainties should arise from the influence of an irregular shape, when more extensive photometric data derived from the different apparitions are used to analyze the photometric phase curve of (106) Dione.

In order to solve this problem, the more extensively applicable brightness model introduced in Section 3.1 can be adopted. Photometric observational data of asteroid (106) Dione were derived in the range of phase angles from 1.0° to 13.1°. Therefore, the morphology of the photometric phase curve of (106) Dione can be characterized and the phase function system parameters can be estimated: absolute magnitude $H = 7.66$ mag, and phase function parameters $G_1 = 0.682$ and $G_2 = 0.081$. The absolute magnitude of 7.66 mag is consistent with the result suggested by Shevchenko & Tedesco (2006). In addition, based on $H = 7.66$ mag and albedo $p_v = 0.07$ (Ryan et al. 2015), a mean size of 148 ± 11 km can be estimated by the relation (Muinonen et al. 2010),

$$\log_{10} D = 3.1236 - 0.2H - 0.5 \log_{10} (p_v). \quad (17)$$

Furthermore, for (106) Dione, based on the values of phase function parameters G_1 and G_2, three additional parameters: phase integral $q = 0.3516$, photometric phase coefficient $k = -1.7679$ and amplitude of the opposition effect $\zeta - 1 = 0.3106$ can be evaluated in terms of the relations derived by Muinonen et al. (2010).

6 CONCLUSIONS

Photometric phase curves for the majority of small solar system bodies have been analyzed with the $H - G$ system or the $H - G_1 - G_2$ system by assuming spherical shapes of asteroids in early studies. Therefore, some errors arising from their non-spherical shapes were introduced into the determinations of phase function system parameters, when the analyzed photometric observational data were derived from different apparitions. In the study of the photometric phase curve of asteroid (107) Camilla (Wang et al. 2016), brightness variations were considered by changes in illuminated and visible cross-sectional area of the tri-axial ellipsoid shape of (107) Camilla, when the viewing aspect angles varied. However, this tri-axial ellipsoid shape model is inappropriate for approximating Dione's quite asymmetric shape. Therefore, a more complicated shape model, the cellinoid ellipsoid, is adopted in the new brightness model of the photometric phase curve. Using this new brightness model, the absolute magnitude H and phase function parameters G_1 and G_2 of (106) Dione are estimated efficiently, and its spin parameters and cellinoid shape are also obtained at the same time. Therefore, our new model can be used to analyze the photometric phase curves and simultaneously to determine the spin parameters and rough shapes of asteroids by utilizing photometric data, which can be collected during multiple apparitions. Finally, this model can be used to investigate the brightness behaviors of more asteroids and enlarge the sample of photometric phase curves in the future.

Acknowledgements We thank the referees for their insightful comments and suggestions that lead to significant improvements in this work. We gratefully acknowledge the computing time granted by Yunnan Observatories and provided on the facilities at the Yunnan Observatories Supercomputing Platform. This work is funded by the National Natural Science Foundation of China (Grant Nos. 11073051, 11473066 and 11673063) and by the Open Project of Key Laboratory of Space Object and Debris Observation, Chinese Academy of Sciences (title: Photometric study of space debris in near geostationary orbit).

References

Belskaya, I. N., & Shevchenko, V. G. 2000, Icarus, 147, 94
Bowell, E., Hapke, B., Domingue, D., et al. 1989, in Asteroids II, ed. R. P. Binzel, T. Gehrels, & M. S. Matthews, 524
Cellino, A., Zappala, V., & Farinella, P. 1989, Icarus, 78, 298
Collier Cameron, A., Wilson, D. M., West, R. G., et al. 2007, MNRAS, 380, 1230
Dlugach, Z. M., & Mishchenko, M. I. 1999, Solar System Research, 33, 472
Dlugach, Z. M., & Mishchenko, M. I. 2013, Solar System Research, 47, 454
Dymock, R., & Miles, R. 2009, Journal of the British Astronomical Association, 119, 149
Gilks, W. R., Richardson, S., & Spiegelhalter, D. J. 1996, Markov Chain Monte Carlo in Practice (Chamman and Hall/CRC)
Hapke, B. 1984, Icarus, 59, 41
Hapke, B. 1986, Icarus, 67, 264
Hapke, B. 2002, Icarus, 157, 523
Harris, A. W., Young, J. W., Dockweiler, T., et al. 1992, Icarus, 95, 115
Kaasalainen, M., Torppa, J., & Muinonen, K. 2001, Icarus, 153, 37
Lu, X., Zhao, H., & You, Z. 2014, Earth Moon and Planets, 112, 73
Lumme, K., & Bowell, E. 1981, AJ, 86, 1694
Michel, P., DeMeo, F. E., & Bottke, W. F. 2015, Asteroids: Recent Advances and New Perspectives, eds. W. F. Bottke, Jr., A. Cellino, P. Paolicchi et al., (University of Arizona Press), 3
Muiños, J. L., & Evans, D. W. 2014, Astronomische Nachrichten, 335, 367
Muinonen, K. 1994, in IAU Symposium, 160, Asteroids, Comets, Meteors 1993, eds. A. Milani, M. di Martino, & A. Cellino, 271
Muinonen, K., Belskaya, I. N., Cellino, A., et al. 2010, Icarus, 209, 542
Muinonen, K., Penttilä, A., Cellino, A., et al. 2009, Meteoritics and Planetary Science, 44, 1937
Muinonen, K., Piironen, J., Shkuratov, Y. G., Ovcharenko, A., & Clark, B. E. 2002, Asteroid Photometric and Polarimetric Phase Effects, eds. W. F. Bottke, Jr., A. Cellino, P. Paolicchi et al. (University of Arizona Press), 123
Oszkiewicz, D. A., Bowell, E., Wasserman, L. H., et al. 2012, Icarus, 219, 283
Penttilä, A., Shevchenko, V. G., Wilkman, O., & Muinonen, K. 2016, Planet. Space Sci., 123, 117
Pray, D. P. 2005, Minor Planet Bulletin, 32, 48
Ryan, E. L., Mizuno, D. R., Shenoy, S. S., et al. 2015, A&A, 578, A42
Shevchenko, V. G., & Tedesco, E. F. 2006, Icarus, 184, 211
Shevchenko, V. G., Belskaya, I. N., Muinonen, K., et al. 2016, Planet. Space Sci., 123, 101
Sykes, M. V., Cutri, M., R., Skrutskie, M. F., et al. 2010, NASA Planetary Data System, 125
Wang, Y.-B., Wang, X.-B., & Wang, A. 2016, RAA (Research in Astronomy and Astrophysics), 16, 015